Electronic Supplementary Information (ESI)

QSAR Study on the Inhibition Mechanism of Matrix Metalloproteinase-12 by Arylsulfone Analogs Based on Molecular Orbital Calculations

Seiji Hitaoka,[a] Hiroshi Chuman,[b,*] and Kazunari Yoshizawa[a,*]

[a]Institute for Materials Chemistry and Engineering and International Research Center for Molecular System, Kyushu University, Fukuoka 819-0395, Japan

[b]Institute of Health Biosciences, The University of Tokushima Graduate School, 1-78 Shomachi, Tokushima 770-8505, Japan

*E-mail: hchuman@tokushima-u.ac.jp
*E-mail: kazunari@ms.ifoc.kyushu-u.ac.jp

List of Contents:

Table S1 Structural data for the docked and experimental geometries around the catalytic zinc ion block

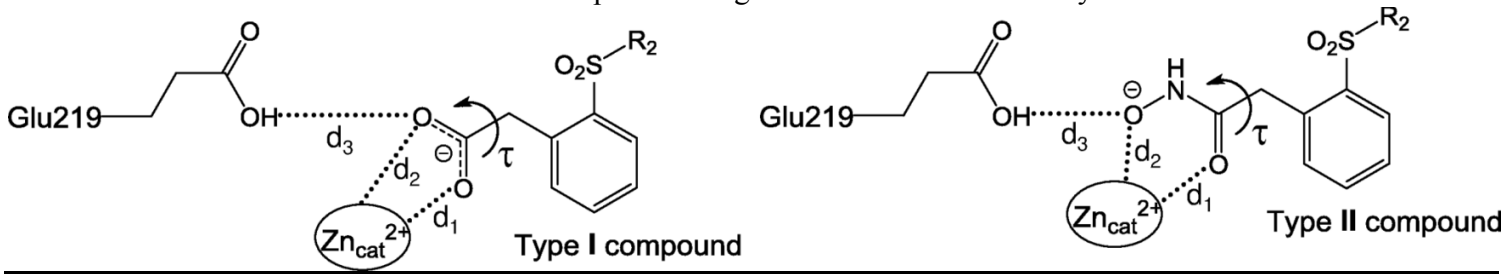

compound		d_1[a]		d_2[a]		d_3[a]		τ[a]	
no.	type	first[b]	top 10[c,d]	first[b]	top 10[c,d]	first[b]	top 10[c,d]	first[b]	top 10[c,d]
1	**I**	2.21	2.22 (0.01)	2.25	2.26 (0.01)	3.16	3.30 (0.32)	81.13	111.13 (38.68)
2	**I**	2.23	2.23 (0.01)	2.23	2.25 (0.01)	3.21	3.21 (0.34)	83.69	135.29 (38.33)
3	**I**	2.20	2.21 (0.01)	2.24	2.26 (0.01)	3.29	3.09 (0.13)	88.22	137.46 (51.61)
4	**I**	2.19	2.21 (0.01)	2.24	2.25 (0.01)	3.31	3.10 (0.17)	89.36	125.91 (47.60)
5	**II**	2.17	2.19 (0.06)	2.51	2.40 (0.09)	2.59	2.60 (0.02)	13.67	23.30 (13.72)
6	**II**	2.16	2.22 (0.07)	2.55	2.93 (1.08)	2.60	3.09 (0.81)	22.39	73.82 (75.57)
7	**II**	2.16	2.19 (0.05)	2.64	2.92 (1.12)	2.59	3.24 (0.87)	24.32	125.23 (109.47)
8	**II**	2.16	2.18 (0.04)	2.53	2.91 (1.12)	2.59	3.34 (0.88)	24.07	129.76 (122.17)
calculated structure[c,e]	**I**	2.22 (0.01)		2.25 (0.01)		3.18 (0.27)		127.45 (45.62)	
	II	2.20 (0.06)		2.79 (0.98)		3.07 (0.79)		88.03 (100.46)	
crystallographic structure[c,f]	**I**	1.99 (0.16)		2.71 (0.17)		2.62 (0.06)		48.55 (17.67)	
	II	2.12 (0.16)		2.20 (0.11)		2.71 (0.19)		61.32 (10.62)	

[a] $d_{1–3}$ (Å) and τ (deg) are distances and angles defined in the insert figure, respectively.

[b] Value of the first ranked structure.

[c] Average value and standard deviation (in parentheses).

[d] Average values of the top 10 ranked complex structures.

[e] Average values of the complex structures for types **I** and **II** compounds.

[f] Average values were obtained from the crystallographic structures of MMP-12–ligand complexes (PDB codes: 1ROS, 3EHX, 3EHY, 3TS4, 4EFS, 4H84, 4I03, and 4H30 (type **I**); 1RMZ, 1YCM, 1Z3J, 2W0D, 2W08, 2W09, 2W0A, 3F1A, 3F15, 3F16, 3F17, 3F18, 3F19, 3LK8, 3N2U, 3N2V, 3NX7, 3RTS, 3RTT, 4GUY, 1JIZ, 1JK3, 4H49, and 4H76 (type **II**)).

Table S2 Representative energy terms (kcal/mol) obtained from the time-average complexes of compounds (a) **2** and (b) **6** for the MD simulations

(a)	compound **2**			
last *t* (ps)	$\Delta E_{bind}^{ONIOM/HF/ME}$	ΔG_{sol}^{polar}	$\Delta E_{bind}^{ONIOM/HF/ME} + \Delta G_{sol}^{polar}$	E_{disp} [a]
200	−304.96 (2.07)[b]	272.70 (2.34)[b]	−32.26 (0.20)[b]	−94.8 (0.18)[b]
300	−306.83 (2.06)[b]	273.19 (2.34)[b]	−33.64 (0.19)[b]	−93.7 (0.18)[b]
400	−305.06 (2.07)[b]	273.21 (2.34)[b]	−31.85 (0.20)[b]	−96.1 (0.18)[b]
single minimized structure	−299.30	266.65	−32.65	−94.7

(b)	compound **6**			
last *t* (ps)	$\Delta E_{bind}^{ONIOM/HF/ME}$	ΔG_{sol}^{polar}	$\Delta E_{bind}^{ONIOM/HF/ME} + \Delta G_{sol}^{polar}$	E_{disp} [a]
200	−331.57 (2.41)[b]	285.43 (2.32)[b]	−46.14 (2.95)[b]	−100.3 (0.62)[b]
300	−328.45 (2.43)[b]	283.12 (2.34)[b]	−45.33 (3.01)[b]	−101.5 (0.61)[b]
400	−333.88 (2.40)[b]	287.34 (2.31)[b]	−46.54 (2.93)[b]	−99.9 (0.62)[b]
single minimized structure	−339.30	291.93	−47.37	−101.2

[a] Lennard−Jones R^{-6} energy term in Amber force field.

[b] A value in parentheses is the relative absolute error (%), which is defined as the absolute difference between energies of the single (only MM) and average (MD + MM) minimized complexes divided by the absolute individual energy term.

Table S3 RMSD values (Å) between the first ranked pose (highest docking score) and the other top 10 ranked poses

pose	compound no.							
	1	**2**	**3**	**4**	**5**	**6**	**7**	**8**
1 (first ranked)	—	—	—	—	—	—	—	—
2	0.65	0.37	0.38	0.35	0.34	0.86	2.75	0.87
3	0.40	0.99	0.35	0.89	0.59	0.32	2.47	2.85
4	0.44	0.96	1.03	0.94	0.91	1.77	2.39	3.24
5	0.64	0.35	1.08	0.61	0.70	1.93	3.21	3.08
6	0.72	0.47	0.82	2.83	1.33	1.88	2.98	3.15
7	0.60	0.56	0.61	0.98	0.91	2.09	2.94	2.09
8	0.44	0.45	0.66	0.36	1.66	0.67	3.12	2.96
9	0.62	0.97	2.97	0.48	1.87	1.02	2.73	2.90
10	1.01	1.01	0.81	0.61	1.98	1.49	2.97	3.41

Table S4 Overall free-energy change ΔG and representative energy terms[a] for compounds in the external test set

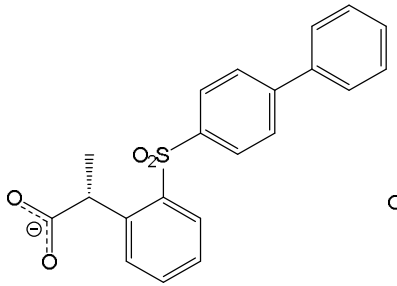

Compound **9** (IC_{50} = 1900 nM)

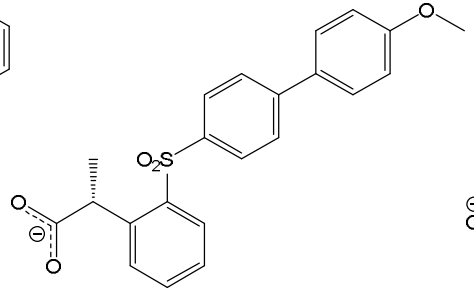

Compound **10** (IC_{50} = 310 nM)

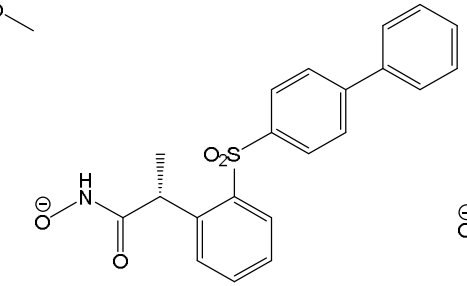

Compound **11** (IC_{50} = 6.0 nM)

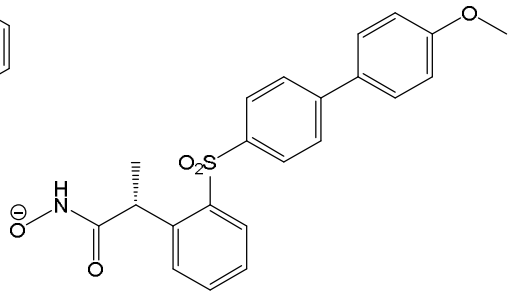

Compound **12** (IC_{50} = 2.7 nM)

compound										
no.	type	ΔG_{obs}[b]	ΔG_{pred}[c]	ΔG_{pred}[d]	ΔG_{pred}[e]	$\Delta E_{bind}^{ONIOM/HF/ME}$	$\Delta E_{bind}^{ONIOM/HF/EE}$	$\Delta E_{bind}^{FMO/HF}$	ΔG_{sol}^{polar}	E_{disp}
9	**I**	−8.12	−8.37	−8.33	−8.41	−299.96	−291.51	−294.24	266.50	−78.45
10	**I**	−9.23	−9.07	−8.91	−9.31	−301.60	−292.55	−297.59	270.35	−83.76
11	**II**	−11.66	−12.83	−12.59	−11.78	−343.17	−333.08	−335.71	290.13	−78.61
12	**II**	−12.15	−13.37	−13.15	−12.72	−342.05	−331.94	−337.17	291.94	−83.97
r_{pred}[f]			0.861	0.908	0.981					

[a] In kcal/mol.

[b] $\Delta G_{obs} = RT \ln IC_{50}$ (T = 310 K). IC_{50} values were obtained as racemates (ref 42).

[c] Predicted from eqn (6).

[d] Predicted from eqn (7).

[e] Predicted from eqn (8).

[f] Predictive correlation coefficient.

Table S5 IFIED (arylsulfone inhibitor, Zn_{cat}^{2+} block) and ΣIFIED values[a]

compound				
no.	type	IFIED (arylsulfone inhibitor, Zn_{cat}^{2+} block)[b]	ΣIFIED[c]	contribution (%)[d]
1	**I**	−235.02	−366.31	64.16
2	**I**	−236.99	−389.60	60.83
3	**I**	−237.41	−373.46	63.57
4	**I**	−237.73	−384.65	61.80
5	**II**	−268.53	−413.40	64.96
6	**II**	−271.98	−437.48	62.17
7	**II**	−275.47	−423.36	65.07
8	**II**	−272.71	−427.91	63.73

[a] In kcal/mol.

[b] IFIED (arylsulfone inhibitor, Zn_{cat}^{2+} block) = E(arylsulfone inhibitor−Zn_{cat}^{2+} block) − [E(arylsulfone inhibitor) + E(Zn_{cat}^{2+} block)].

[c] ΣIFIED represents the sum of the IFIED values for all the fragments.

[d] Percentage of IFIED (arylsulfone inhibitor, Zn_{cat}^{2+} block) in ΣIFIED.

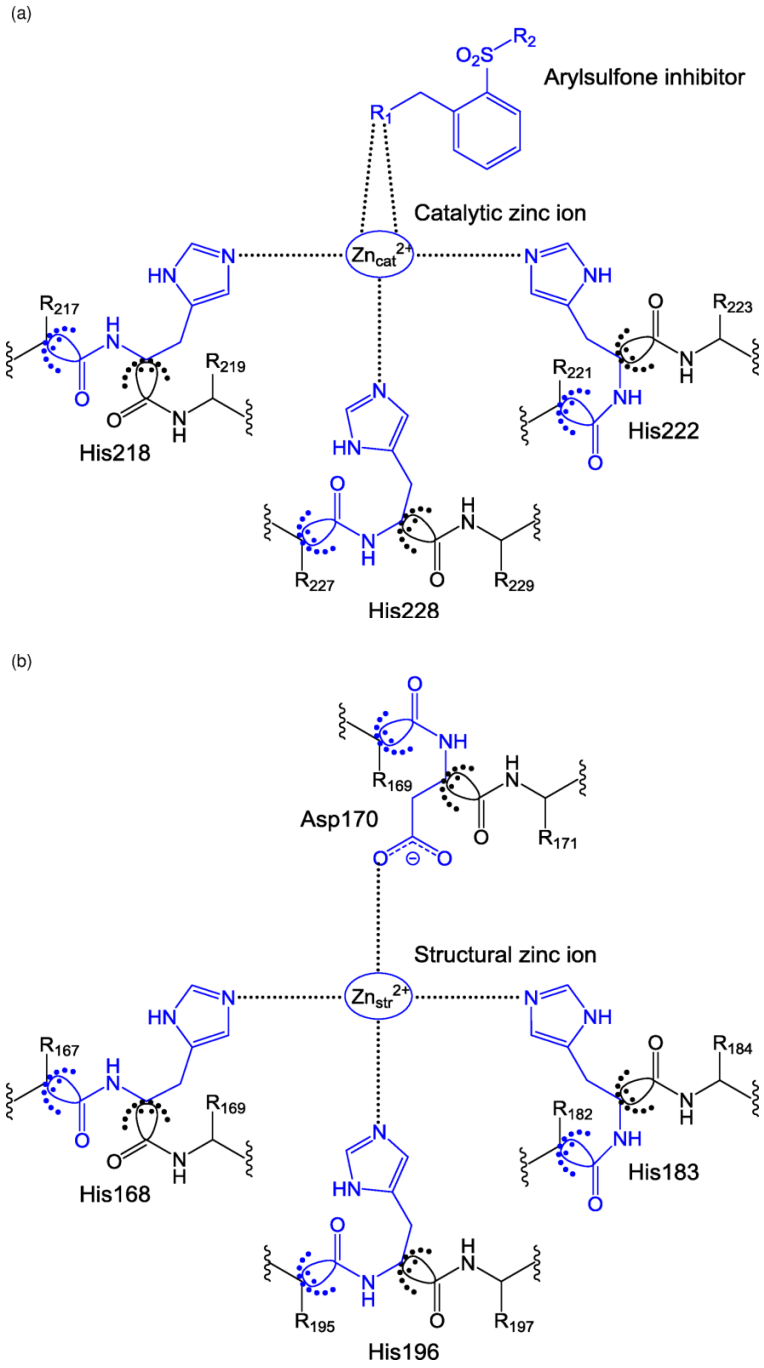
(a)
Arylsulfone inhibitor
Catalytic zinc ion
His218
His222
His228
(b)
Asp170
Structural zinc ion
His168
His183
His196

(c)

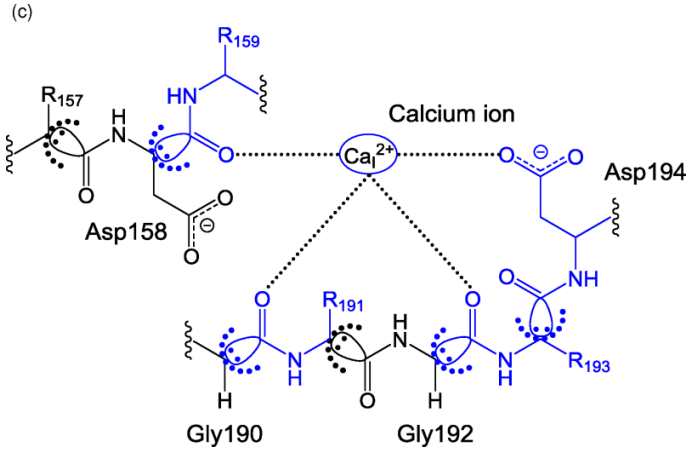
R159
HN
R157
H
N
Calcium ion
Ca$_I^{2+}$
Asp194
Asp158
NH
R191
R193
Gly190
Gly192

(d)

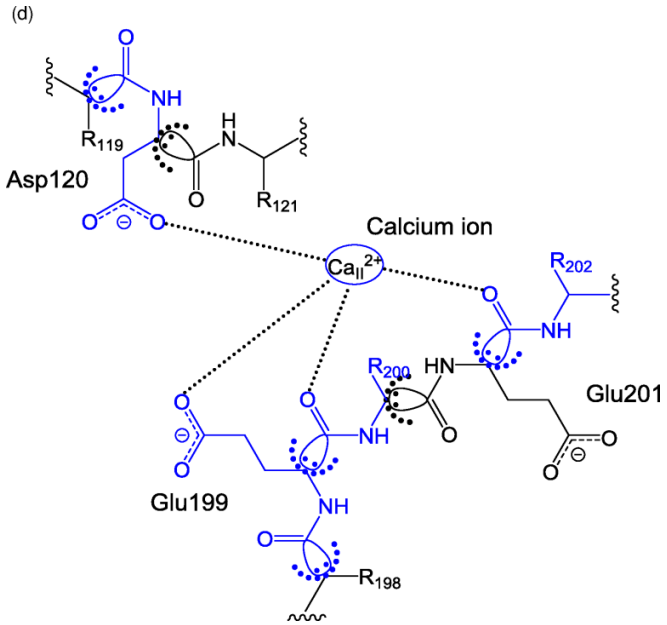
NH
R119
Asp120
R121
Calcium ion
Ca$_{II}^{2+}$
R202
NH
R200
HN
Glu201
Glu199
NH
R198

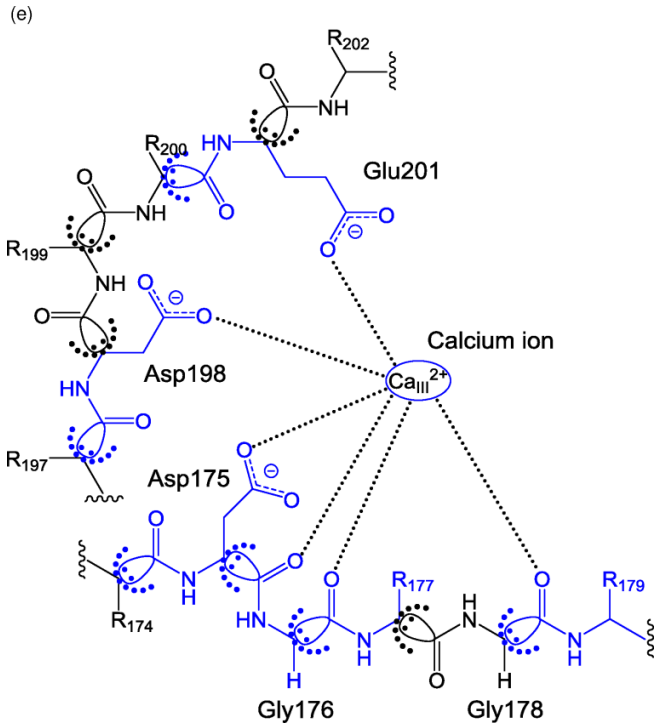

Fig. S1 FMO fragmentation of ion blocks : (a) Zn_{cat}^{2+}, (b) Zn_{str}^{2+}, (c) Ca_{I}^{2+}, (d) Ca_{II}^{2+}, and (e) Ca_{III}^{2+} blocks. Atoms shown in blue are combined together and treated as a single FMO fragment in FMO calculations. The catalytic zinc ion block (Zn_{cat}^{2+} block: Zn_{cat}^{2+}, His218, His222, and His228) and an arylsulfone inhibitor were combined and treated as a single FMO fragment (arylsulfone inhibitor–Zn_{cat}^{2+} block) to avoid the convergence problem in the FMO calculations. The similar treatment was applied to the structural zinc ion block (Zn_{str}^{2+} block: Zn_{str}^{2+}, His168, His183, His196, and Asp170) and three calcium ion blocks. FMO-fragments (including the binding water molecule) other than two Zn^{2+} and three Ca^{2+} blocks were taken as one residue.

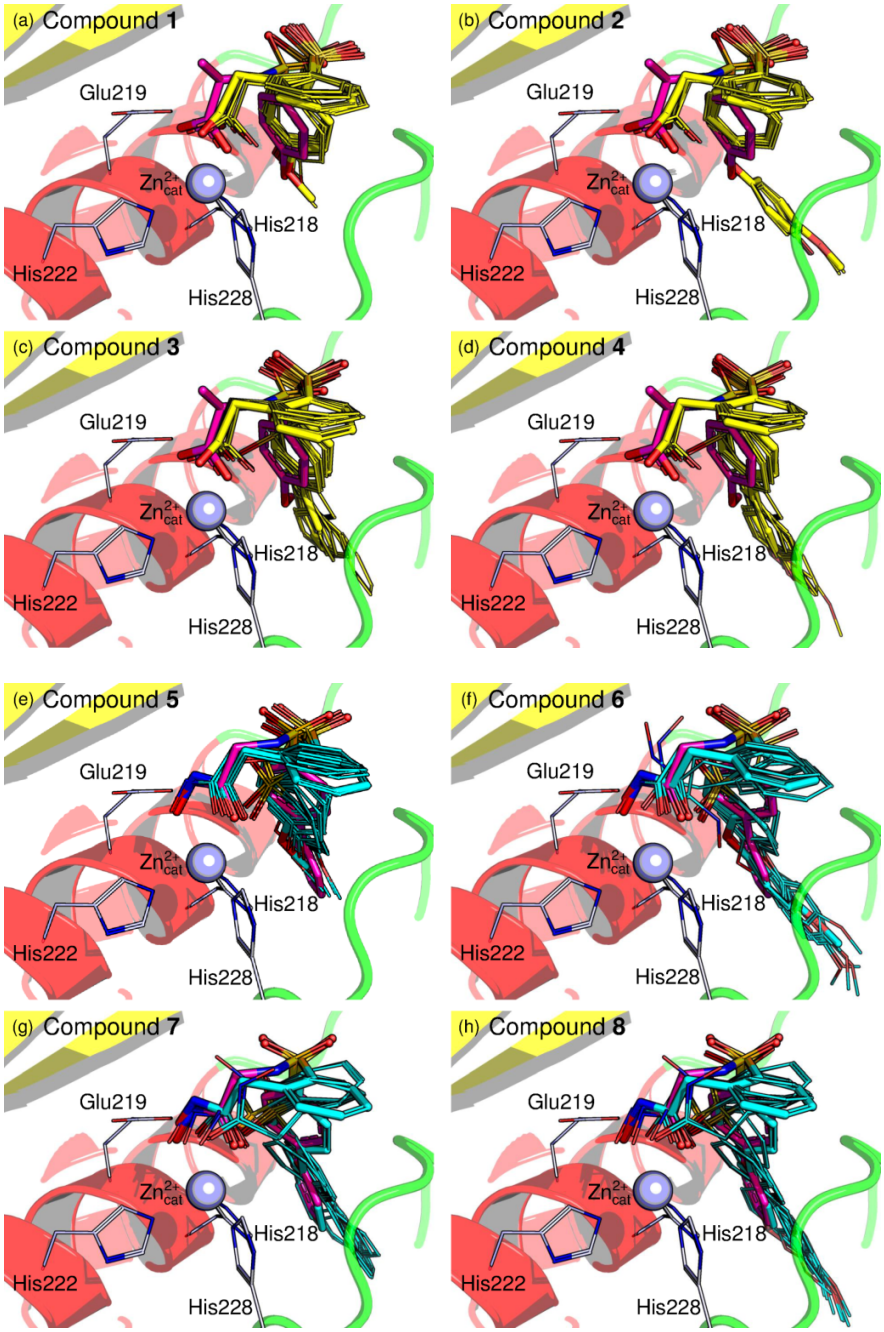

Fig. S2 Comparison between the docked (top 10 ranked) and crystallographically observed binding modes of the zinc binding groups. Superimpositions of the X-ray structure of the carboxylic acid zinc binding group based ligand (PDB code: 3EHY) and the type **I** compounds (a) **1**, (b) **2**, (c) **3**, and (d) **4**. Superimpositions of the X-ray structure of the hydroxamic acid zinc binding group based ligand (3F17) and the type **II** compounds (e) **5**, (f) **6**, (g) **7**, and (h) **8**. The X-ray and first ranked types **I** and **II** structures are represented in a stick model with magenta, yellow, and cyan, respectively. The other docked structures are represented in a line model.

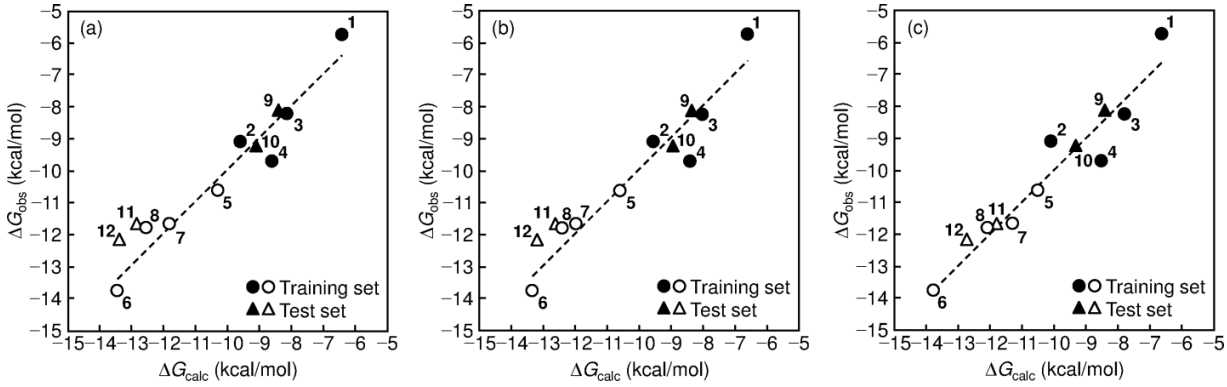

Fig. S3 Plots of ΔG_{obs} with ΔG_{calc} for the training (internal) and test (external) sets obtained from the LERE-QSAR equations (a) (6), (b) (7), and (c) (8). Solid and open symbols represent types **I** and **II** compounds, respectively.

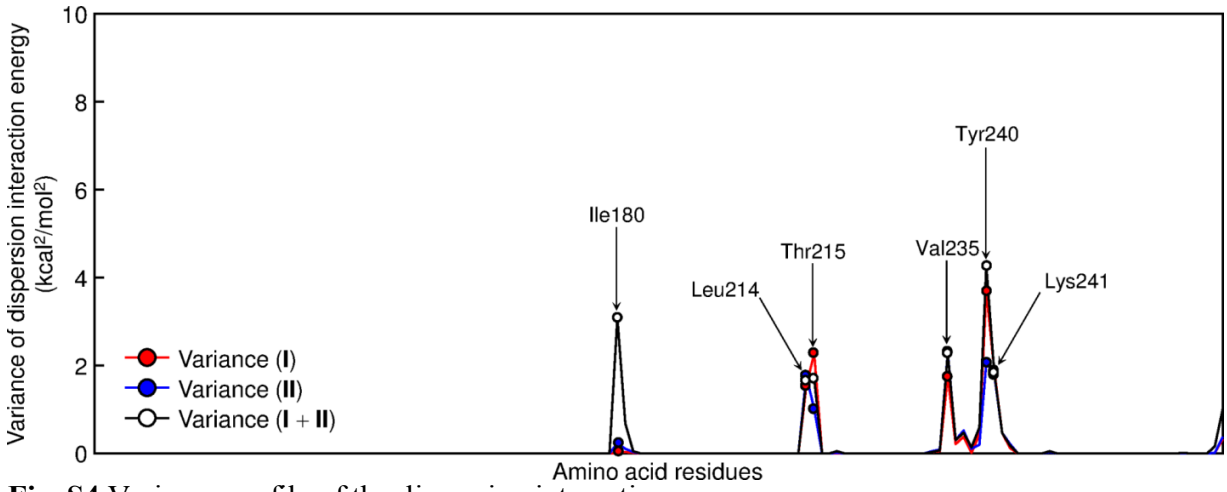

Fig. S4 Variance profile of the dispersion interaction energy.